



Published in final edited form as:

Exp Eye Res. 2021 December ; 213: 108846. doi:10.1016/j.exer.2021.108846.

Hyperglycemia-induced effects on glycocalyx components in the retina

Gaganpreet Kaur¹, Janet Rogers², Nabil A. Rashdan¹, Diana Cruz-Topete¹, Christopher B. Pattillo¹, Steve Hartson², Norman R. Harris¹

¹Louisiana State University Health Science Center-Shreveport, LA, Department of Molecular and Cellular Physiology

²Oklahoma State University, OK, Department of Biochemistry and Molecular Biology

Abstract

Purpose: Diabetic retinopathy is a vision-threatening complication of diabetes characterized by endothelial injury and vascular dysfunction. The loss of the endothelial glycocalyx, a dynamic layer lining all endothelial cells, contributes to several microvascular pathologies, including an increase in vascular permeability, leukocyte plugging, and capillary occlusion, and may drive the progression of retinopathy. Previously, a significant decrease in glycocalyx thickness has been observed in diabetic retinas. However, the effects of diabetes on specific components of the retinal glycocalyx have not yet been studied. Therefore, the aim of our study was to investigate changes in synthesis, expression, and shedding of retinal glycocalyx components induced by hyperglycemia, which could provide a novel therapeutic target for diabetic retinopathy.

Methods: Primary rat retinal microvascular endothelial cells (RRMEC) were grown under normal glucose (5 mM) or high-glucose (25 mM) conditions for 6 days. The mRNA and protein levels of the glycocalyx components were examined using qRT-PCR and Western blot analysis, respectively. Further, mass spectrometry was used to analyze protein intensities of core proteins. In addition, the streptozotocin-induced Type 1 diabetic rat model was used to study changes in the expression of the retinal glycocalyx *in vivo*. The shedding of the glycocalyx was studied in both culture medium and in plasma using Western blot analysis.

Results: A significant increase in the shedding of syndecan-1 and CD44 was observed both *in vitro* and *in vivo* under high-glucose conditions. The mRNA levels of syndecan-3 were significantly lower in the RRMEC grown under high glucose conditions, whereas those of syndecan-1, syndecan-2, syndecan-4, glypican-1, glypican-3, and CD44 were significantly higher. The protein expression of syndecan-3 and glypican-1 in RRMEC was reduced considerably following exposure to high glucose, whereas that of syndecan-1 and CD44 increased significantly.

Corresponding Author: Norman R. Harris, Professor and Chair, Department of Molecular and Cellular Physiology, Louisiana State University Health Science Center-Shreveport, 1501 Kings Highway, Shreveport, LA 71103, norman.harris@lsuhs.edu.

Publisher's Disclaimer: This is a PDF file of an unedited manuscript that has been accepted for publication. As a service to our customers we are providing this early version of the manuscript. The manuscript will undergo copyediting, typesetting, and review of the resulting proof before it is published in its final form. Please note that during the production process errors may be discovered which could affect the content, and all legal disclaimers that apply to the journal pertain.

Conflicts of Interest

The authors have no conflicts of interest to disclose.

In addition, mass spectrometry data also suggests a significant increase in syndecan-4 and a significant decrease in glypican-3 protein levels with high glucose stimulation. *In vivo*, our data also suggest a significant decrease in the mRNA transcripts of syndecan-3 and an increase in mRNA levels of glypican-1 and CD44 in the retinas of diabetic rats. The diabetic rats exhibited a significant reduction in the retinal expression of syndecan-3 and CD44. However, the expression of syndecan-1 and glypican-1 increased significantly in the diabetic retina.

Conclusions: One of the main findings of our study was the considerable diversity of glucose-induced changes in expression and shedding of various components of endothelial glycocalyx, for example, increased endothelial and retinal syndecan-1, but decreased endothelial and retinal syndecan-3. This indicates that the reported decrease in the retinal glycocalyx in diabetes is not a result of a non-specific shedding mechanism. Moreover, mRNA measurements indicated a similar diversity, with increases in endothelial and/or retinal levels of syndecan-1, glypican-1, and CD44, but a decrease for syndecan-3, with these increases in mRNA potentially a compensatory reaction to the overall loss of glycocalyx.

Keywords

Diabetes; Hyperglycemia; Retina; Glycocalyx; Syndecans; Glypicans; CD44; Endothelial Cells

1. Introduction

The global prevalence of diabetes is increasing at an alarming rate. Currently, 463 million people worldwide have diabetes, which is projected to increase to 700 million by 2045 (Saeedi et al., 2019). According to the American Diabetes Association, 10.5% of the US population is suffering from diabetes (ADA). Diabetic retinopathy (DR), one of the major complications of diabetes, affects one third of diabetic patients and is the most common cause of blindness among adults (CDC). Hyperglycemia, an important feature of Type 1 and Type 2 diabetes, causes vascular dysfunction, inflammation, and neurodegeneration in the retina (Gui, You, Fu, Wu, & Zhang, 2020). Together, these events cause endothelial cell injury and break down the blood-retinal barrier, which can lead ultimately to the formation of acellular capillaries and edema in the retinal vasculature (Gui et al., 2020). The damage to blood vessels leads to ischemia and abnormal neovascularization, which increases DR severity and eventually causes vision impairment (Wright, Eshaq, Lee, Kaur, & Harris, 2020). Previously, we have shown an altered distribution of red blood cells in the diabetic retina, with a reduced fraction arriving in the deep capillary layer and increased flow shunting towards the superficial vascular layer (Leskova, Watts, Carter, Eshaq, & Harris, 2013). Several treatments and therapies are available, including anti-VEGF agents, laser photocoagulation, and intravitreal corticosteroids, that can halt further deterioration of vision if administered in a timely manner (Simó & Hernández, 2015). However, prolonged use of corticosteroids has been linked to cataract formation and increased intraocular pressure (Simó & Hernández, 2015). In addition, laser photocoagulation is associated with loss of peripheral vision and visual acuity and changes in color vision (Simó & Hernández, 2015). Anti-VEGF agents are the first-line therapy for DR; however, they are expensive, require frequent injection, and are not universally effective (Simó & Hernández, 2015; W. Wang & Lo, 2018). New insight into the molecular mechanism underlying the early stage of

DR is required to identify alternative therapeutic targets. It is possible that the loss of the endothelial glycocalyx could contribute to the microvascular complications present in DR.

The endothelial glycocalyx is a carbohydrate-rich mesh-like network present on the vascular endothelium (Reitsma, Slaaf, Vink, van Zandvoort, & oude Egbrink, 2007). The major backbone molecules of the glycocalyx are proteoglycans, which themselves are composed of core proteins and covalently attached glycosaminoglycan chains (GAGs) (Reitsma et al., 2007). The central core proteins are either transmembrane proteins from the syndecan family or the GPI-anchored glypican family. Each syndecan has an extracellular domain, a single-span transmembrane domain, and a short cytoplasmic tail (Tkachenko, Rhodes, & Simons, 2005). Heparan sulfate (HS) and chondroitin sulfate (CS), two major GAGs, are found on the extracellular domain of core proteoglycans, whereas hyaluronic acid (HA) binds to its receptors, mainly CD44 (a transmembrane glycoprotein) (Hasib et al., 2019; Reitsma et al., 2007).

The glycocalyx is a crucial regulator of vascular permeability; it limits the passage of plasma molecules to the endothelial cell membrane using steric hindrance and electrostatic charge (the glycocalyx is negatively charged due to sulfated molecules) (Reitsma et al., 2007). Enzymatic degradation of the glycocalyx has been shown to increase retinal vascular leakage (Leskova et al., 2019), a major microvascular complication of DR. In addition, the glycocalyx affects blood cell and vessel wall interactions (Reitsma et al., 2007). The removal of the endothelial glycocalyx by infusion of ox-LDL and heparitinase causes the increased adhesion of platelets and leukocytes to the endothelium, respectively (Constantinescu, Vink, & Spaan, 2003; Vink, Constantinescu, & Spaan, 2000). Adherent leukocytes have been temporally and spatially linked with retinal endothelial cell injury and death in an experimental rat model of diabetes (Joussen et al., 2001). Both computational and *in vivo* studies have shown that the absence of the glycocalyx at the vessel wall impairs perfusion and red blood cell flux (Cabral, Vazquez, Tsai, & Intaglietta, 2007; McClatchey, Schafer, Hunter, & Reusch, 2016). Syndecan-1, syndecan-3, and glypican-1 have shown to regulate major endothelial function including permeability, leukocyte adhesion, shear stress-induced eNOS activation, angiogenesis, and anchoring of tissue factor pathway inhibitor (Arokiasamy, Balderstone, De Rossi, & Whiteford, 2019; Bartosch, Mathews, & Tarbell, 2017; Ebong, Lopez-Quintero, Rizzo, Spray, & Tarbell, 2014; Götte et al., 2002; Qing et al., 2015; Tinholt et al., 2015). Therefore, alterations in proteoglycan levels can cause endothelial dysfunction which may contribute to the pathogenesis of DR.

It has been suggested that endothelial glycocalyx perturbations in diabetes are involved in the initiation of systemic vascular complications (Nieuwdorp, Mooij, et al., 2006). The volume of systemic glycocalyx decreased more than 60% along with increased shedding of glycocalyx components in the plasma of Type 1 diabetic patients compared to that of healthy volunteers (Nieuwdorp, Mooij, et al., 2006). In healthy individuals, an acute hyperglycemic clamp (a glucose concentration of 300 mg/dL) for 6 hours significantly reduced (~50%) the glycocalyx volume, which was prevented when N-acetylcysteine (a free radical scavenger) was infused along with hyperglycemic clamp (Nieuwdorp, van Haefen, et al., 2006). Using electron microscopy, Kumase et al. showed a 50% decrease in the glycocalyx thickness in the retinas of rats in a streptozotocin (STZ) induced Type 1 diabetes model (Kumase et

al., 2010). Similarly, using the two-dye infusion technique, Broekhuizen et al. showed the same percentage reduction in the thickness of the retinal endothelial glycocalyx of Type 2 diabetic patients (Broekhuizen et al., 2010). The glycocalyx thickness in diabetic patients was partially restored following dietary supplementation for 8 weeks with sulodexide, a mixture of GAGs containing mainly heparan sulfate (80%) and dermatan sulfate (20%) (Broekhuizen et al., 2010). In Ins2(Akita) mice, a genetic model of Type 1 diabetes, we have previously shown a 35% reduction in the retinal arteriolar, but not venular, glycocalyx thickness (Leskova et al., 2019).

Although glycocalyx thickness has been shown to significantly decrease in the diabetic retina, the effect of high glucose on the specific composition of the retinal glycocalyx is not well studied. One study has reported a significant reduction in the synthesis of heparan sulfate and mRNA levels of perlecan, the latter being a proteoglycan primarily found on the basement membrane (Noonan et al., 1991), 20 weeks after the induction of diabetes in Wistar rats using STZ (Bollineni, Alluru, & Reddi, 1997). Given the critical nature of the roles of glycocalyx proteoglycans in endothelial function, we investigated the effect of hyperglycemia on the retinal synthesis, expression, and shedding of core proteins, mainly syndecan-1, syndecan-3, glypican-1, and CD44, using STZ-induced Type 1 diabetic rats.

2. Materials and Methods

2.1 *In vitro* model of hyperglycemia

Primary rat retinal endothelial cells (RRMEC) were purchased from Cell Biologics (Chicago, IL) and cultured in Dulbecco's Modified Eagle's Medium (DMEM) containing 5% heat inactivated fetal bovine serum (Atlanta Biologicals, Flowery Branch, GA), 1% GlutaMAX (ThermoFisher Scientific, Waltham, MA), and 1% antibiotic-antimycotic solution (10,000 U/mL penicillin, 10,000 µg/mL streptomycin, and 25 µg/mL Amphotericin B; ThermoFisher Scientific, Waltham, MA). RRMEC monolayers were grown for 6 days either in normal glucose media (DMEM with 5 mM glucose; control conditions) or in high-glucose media (20 mM D-glucose, Sigma-Aldrich, St. Louis, MO, added to DMEM containing 5 mM glucose) in an incubator with 5% CO₂ at 37 °C, with a partial media change on day 3. After 6 days, the culture media and RRMEC were collected for analysis. With only a single partial media exchange, the protein analysis may reflect protein accumulated on any or all of the 6 days of the protocol. All experiments were performed from passages 7 to 9.

2.2 Animal model of Type 1 diabetes

For our animal studies, male Wistar rats (100–120 g) were purchased from Envigo (Indianapolis, IN). The Institutional Animal Care and Use Committee of Louisiana State University Health Science Center-Shreveport approved the animal protocols, and all procedures were performed in compliance with the ARVO statement for the Use of Animals in Ophthalmic and Vision Research.

To establish a Type 1 diabetes model, age-matched Wistar rats were injected with either a vehicle (sodium citrate buffer, pH 4.5, control group) or streptozotocin (30 mg/kg/day, diabetic group; Millipore Sigma, Burlington, MA) for 3 consecutive days. Rats with a

non-fasting glucose level of 150 mg/dL or less were used as controls, while rats exhibiting a non-fasting blood glucose level higher than 300 mg/dL were considered hyperglycemic. To verify constant hyperglycemia, the blood glucose levels were measured at 1, 5, and 8 weeks following STZ injection. Plasma and retinal samples were collected 8 weeks after the induction of hyperglycemia. The rats were anesthetized with ketamine (100 mg/kg) and xylazine (10 mg/kg) and the eyes enucleated for retinal isolation for further analysis. Whole blood was collected via femoral artery cannulation and centrifuged at 5000 rpm for 10 minutes at 4 °C to obtain plasma, which was stored at -80 °C until used for Western blot analysis.

2.3 Western Blot

Retinas and RRMEC were lysed in radioimmunoprecipitation assay (RIPA) buffer containing a protease inhibitor (Sigma-Aldrich, St. Louis, MO). The protein concentrations of cell and retina lysates, plasma, and cell culture medium were determined using the Pierce BCA protein assay (ThermoFisher Scientific, Waltham, MA). The sample buffer (Laemmli buffer, Bio-Rad, Hercules, CA) was added to dilute samples to a final concentration of 1 µg/µL.

Equal amounts of protein (10 µg for syndecan-1 and CD44; 30 µg for syndecan-3 and glypican-1) were loaded and separated using 10% SDS-polyacrylamide gels. The proteins were then transferred to nitrocellulose membranes and blocked using Pierce protein-free blocking buffer (ThermoFisher Scientific, Waltham, MA). The membranes were immunoblotted with primary antibodies : (A) syndecan-1 (1:2000, EPR6454, Abcam, Cambridge, United Kingdom), (B) CD44 (1:2000, EPR18668, Abcam, Cambridge, United Kingdom), (C) syndecan-1 (1:1000, PA5-79961, ThermoFisher, Waltham, MA), and (D) glypican-1 horseradish peroxidase (HRP) conjugated (1:1000, SC-365000 HRP, Santa Cruz Biotechnology, Dallas, TX) overnight at 4 °C. When examining the expression of syndecan-3 and glypican-1 in the retina, the membranes were immunoblotted with their respective primary antibodies for 72 hours. The membranes were then incubated with HRP-conjugated secondary antibody for 1 hour at room temperature (RT) followed by detection of specific bands using an electrochemiluminescent system (Bio-Rad, Hercules, CA). The blots were imaged using the ChemiDoc XRS gel imaging system (Bio-Rad, Hercules, CA) and quantified using Image J (National Institutes of Health, Bethesda, MD). HRP-conjugated β-Actin (1:2000, SC-47778, Santa Cruz Biotechnology, Dallas, TX) was used as loading control for retina and RRMEC samples; Ponceau staining (Sigma, St. Louis, MO) was used as a control for plasma and media samples.

2.4 RNA Isolation

RRMEC and retinas were collected for RNA extraction in RLT buffer (Qiagen, Hilden, Germany) and QIAzol lysis buffer (Qiagen, Hilden, Germany), respectively. Total RNA was isolated using a RNeasy Minikit (Qiagen, Hilden, Germany) and RNase-free DNase I (Qiagen, Hilden, Germany) treatment according to the manufacturer's protocols. RNA quality and concentration were determined using a NanoDrop 100 spectrophotometer (ThermoFisher Scientific, Waltham, MA). RNase-free water was used to dilute the samples

to a final concentration of 25 ng/ μ L. Retinal samples processed for syndecan-1 mRNA analysis were diluted to a final concentration of 50 ng/ μ L.

2.5 qRT-PCR

The mRNA levels of the target genes were quantified using real time-PCR (qRT-PCR) using TaqMan Universal PCR Master Mix, no AmpErase UNG (ThermoFisher Scientific, Waltham, MA). qRT-PCR was carried out at 48 °C for 30 minutes, 95 °C for 10 minutes, 95 °C for 15 seconds, and 60 °C for 1 minute (40 cycles of steps 3 and 4) on a CFX96 or CFX384 (Bio-Rad, Hercules, CA) sequence detection PCR system. The relative expression was calculated using the 2^{-C_t} analysis method with expression normalized to the housekeeping gene peptidylprolyl isomerase B (Ppib). All samples were analyzed in duplicate; qRT-PCR was carried out using 100 ng RNA. The expression of the following genes was evaluated: syndecan-1 (SDC1; Rn00564662_m1), syndecan-3 (SDC3; Rn00588067_m1), syndecan-4 (SDC4; Rn00561900_m1), glypican-1 (GPC1; Rn01290371_m1), and CD44 (CD44; Rn00681157_m1). All probes were purchased from Applied Biosystems (Waltham, MA). The abundance of syndecan-1 mRNA was determined using an iTaq Universal Probes One-Step Kit (Bio-Rad, Hercules, CA) and 200 ng RNA. The reaction was carried out at 50 °C for 10 minutes, 95 °C for 5 minutes, 95 °C for 10 seconds, and 60 °C for 30 seconds (40 cycles of steps 3 and 4).

2.6 Osmolarity treatment

To study the effect of osmolarity on the expression of core proteins in RRMEC, monolayers were grown for 6 days using different osmotic controls with osmolarity equivalent to the high-glucose treatment. Mannitol, L-glucose, and o-methyl-d-glucopyranose were added at a concentration of 20 mM, while NaCl was added at a concentration of 10 mM, to normal glucose media. All chemicals were purchased from Sigma-Aldrich (St. Louis, MO).

2.7 ELISA

The levels of insulin in plasma collected from non-diabetic and diabetic rats and from culture medium (normal glucose and high-glucose medium) were measured using a rat insulin enzyme-linked immunosorbent assay (ELISA; Crystal Chem, Elk Grove Village, IL) according to the manufacturer's instructions.

2.8 Membrane protein isolation

For membrane protein enrichment, the membrane proteins were isolated using a subcellular protein fractionation kit for cultured cells (ThermoFisher Scientific, Waltham, MA) according to the manufacturer's instructions. The protein concentration of the extract was determined using the Pierce BCA protein assay (ThermoFisher Scientific, Waltham, MA). Equal amounts of protein extract (100 μ g) were used for mass spectrometry analysis.

2.9 Mass spectrometry

Mass spectrometry analyses were performed in the Genomics and Proteomics Center at Oklahoma State University. Equal amounts of membrane extract were dissolved in 3%

SDS and processed using S-trap devices according to the manufacturer's protocols (ProtoFi, Farmingdale, NY).

Peptides were separated on an Acclaim PepMap RSLC column (2 μ m C18 particles, 75 μ m ID \times 50 cm length; ThermoFisher Scientific, Waltham, MA) and then developed in 0.1% aqueous formic acid using an acetonitrile gradient from 2.5% to 30% acetonitrile over 120 min. The column terminated with a stainless-steel emitter within a Nanospray Flex ion source (ThermoFisher Scientific, Waltham, MA) coupled to a Fusion mass spectrometer programmed for a Top Speed analysis using quadrupole isolation, HCD fragmentation, and fragment ion analysis in the ion trap sector. The instrument settings are provided in an excel spreadsheet as a supplement.

MaxQuant software (v .6.10.43) (Max Planck Institute of Biochemistry, Munich, Germany) was used for the identification and quantification of the mass spectrometry data set (Cox & Mann, 2008). Data were searched against a database of 29,953 rat protein sequences downloaded from Uniprot on April 1, 2020; searches also included reversed decoy sequences and common laboratory protein contaminants. Searches utilized the MaxQuant defaults, supplemented with the "match between runs" feature. LFQ protein intensities (relative protein abundance) from the MaxQuant search were used to analyze protein expression of glyocalyx components. Relative expression between samples was normalized based on the sum of the peptide intensities in each sample, via the LFQ algorithm in MaxQuant as described previously (Cox et al., 2014; Cox & Mann, 2008). Relative protein intensities (LFQ intensities) in high glucose are normalized against the normal glucose group and data is presented as ratio (fold change) of protein expression normal glucose/high glucose. The description of MS results is provided in Table 1. Sample reproducibility was attested by graphing log 2 LFQ protein intensities from various bio-samples among each other, which ensures that the majority of protein in each MS samples was equivalent between the set of samples.

2.10 Statistics

All statistical analysis was performed using GraphPad Prism 9 software (version 9.1.1). The normality of data sets was tested using a Kolmogorov-Smirnov test or a Shapiro-Wilk test. If the data passed the normality test, they were then analyzed using an unpaired, two-tailed Student's *t*-test (for two groups) or one-way ANOVA (for three or more groups) followed by Dunnett's multiple comparison test. A Mann Whitney *U* test or a Kruskal Wallis test followed by Dunn's multiple comparison test were used to analyze data failing the normality test. Body weight and glucose data sets were analyzed using two-way ANOVA followed by Tukey's multiple comparison test. Except for body weight and glucose measurements (presented as medians), all data are presented as mean \pm SEM. *p* values less than 0.05 (95% confidence interval) were considered statistically significant.

3. Results

3.1 Body weight, blood glucose, and insulin levels of animals

In STZ-injected rats, hyperglycemia was observed along with a significantly lower weight gain. At the beginning of the experiments, the body weight of the rats was similar in both groups; however, 8 weeks post-STZ treatment, the diabetic rats exhibited a significant lower body weight ($p < 0.0001$) compared to the non-diabetic rats (Fig. 1A). As expected, STZ-injected rats demonstrated significantly higher ($p < 0.0001$) blood glucose as compared to controls (Fig. 1B). The glucose meter (AlphaTRAK) used for the analysis displays a maximum reading of 750 mg/dL; therefore, diabetic rats exhibiting 'high' readings on the meter are given values of 750 mg/dL. Despite the large variation, a significant decrease ($p < 0.05$) in plasma insulin levels (measured in a subset of animals) was observed in diabetic rats (0.23 ± 0.09 ng/mL) compared to non-diabetic rats (0.88 ± 0.22 ng/mL) (Fig. 1C).

3.2 Effect of high glucose on syndecan-1

A substantial but non-significant (60%, $p = 0.11$; Fig. 2A) increase in the mRNA levels of syndecan-1 was observed in the retinas of diabetic rats compared to their non-diabetic counterparts. In addition, we observed a significant increase in the protein expression of syndecan-1 in the retinas of diabetic rats compared to controls (80% increase in Western blot intensity, $p < 0.01$; Fig. 2B). Plasma levels of syndecan-1 exhibited a significant increase in mean band density in STZ-injected rats compared with controls (54%, $p < 0.001$; Fig. 2C), indicating increased shedding of syndecan-1 in diabetes.

To analyze the effects of high glucose on the glycocalyx, specifically in the endothelial cells of the retina, RRMEC were incubated with normal glucose (5 mM) or high-glucose (25 mM) media for 6 days. The insulin levels in the culture medium were similar in the normal glucose and high-glucose media (data not provided). Using qRT-PCR, we observed a significant increase (380%, $p < 0.0001$) in the mRNA levels of syndecan-1 in RRMEC treated with high glucose compared to control conditions (Fig. 2D). Consistent with our *in vivo* findings, we observed a significant increase in the immunoblot intensity of syndecan-1 in RRMEC grown in high-glucose media (87% increase, $p < 0.01$; Fig. 2E). Lastly, we found an increase in the syndecan-1 media levels (54.3% increase in mean band density, $p < 0.05$; Fig. 2F) under hyperglycemic conditions, providing further evidence for increased shedding of syndecan-1 in diabetes. Shed syndecan-1 contains intact HS chains (Szatmári, Ötvös, Hjerpe, & Dobra, 2015), which can explain the higher molecular weight of syndecan-1 in plasma and media (131 kD) as compared to retina and cell lysate (31 kD).

3.3 Effect of high glucose on syndecan-3

The retinas of diabetic rats exhibited a significant decrease in both mRNA (24%, $p < 0.05$; Fig. 3A) and protein levels of syndecan-3 (26% decrease in mean band density, $p < 0.05$; Fig. 3B) compared to non-diabetic rats. However, no difference was observed in the plasma levels of syndecan-3 between diabetic and non-diabetic rats (Fig. 3C).

The incubation of RRMEC with high glucose (25 mM) led to a significant reduction in the expression of syndecan-3. Both mRNA transcripts (83%, $p < 0.01$; Fig. 3D) and the protein

immunoblot intensity of syndecan-3 (38%, $p<0.01$; Fig. 3E) decreased significantly under hyperglycemic conditions compared to control conditions. We further observed a significant decrease (32% decrease in mean band density, $p<0.01$; Fig. 3F) in the media level of syndecan-3 following high-glucose treatment.

3.4 Effect of high glucose on glypican-1

Eight weeks of diabetes caused an ~30% increase in glypican-1 mRNA levels in the retinas of diabetic rats compared to controls ($p<0.05$; Fig. 4A). In addition, the retinal Western blot intensity of glypican-1 also increased significantly in diabetic animals (113%, $p<0.001$; Fig. 4B). However, the plasma levels of glypican-1 were not different between diabetic and non-diabetic rats (Fig. 4C).

A significant increase was observed in the mRNA transcripts of glypican-1 in RRMEC stimulated with high glucose (200%, $p<0.0001$; Fig. 4D). However, contrary to our findings *in vivo*, the mean band density of glypican-1 decreased significantly with hyperglycemia in RRMEC (37.3%, $p<0.0001$; Fig. 4E). We observed a trend (non-significant) for an increase (32%, $p=0.09$; Fig. 4F) in the Western blot intensity of glypican-1 levels in culture medium following high-glucose treatment.

3.5 Effect of high glucose on CD44

qRT-PCR analysis of the retinas of diabetic rats revealed a significant increase in mRNA levels of CD44 compared to controls (~27%, $p<0.01$; Fig. 5A). However, the retinal mean band density of CD44 protein decreased significantly in diabetic animals (25%, $p<0.001$; Fig. 5B). Furthermore, compared to non-diabetic animals, diabetic rats exhibited a significantly higher Western blot intensity of soluble CD44 in the plasma (52% increase, $p<0.05$; Fig. 5C), demonstrating increased shedding of CD44 into the circulation.

RRMEC monolayers grown in high glucose had a significant increase in both mRNA (75%, $p<0.05$; Fig. 5D) and protein immunoblot intensity of CD44 (19%, $p<0.05$; Fig. 5E) as compared to the monolayers grown in normal glucose. In addition, hyperglycemic conditions led to an increase in mean band density of the CD44 levels in culture medium (~118%, $p<0.05$; Fig. 5F), providing further evidence of increased shedding of CD44 in diabetes.

3.6 Effect of osmolarity of core proteins in RRMEC

High-glucose medium has a higher osmolarity than normal glucose medium. Therefore, to determine whether osmolarity plays a role in hyperglycemia-induced changes in glycocalyx expression, the monolayers were grown using several different osmotic controls (mannitol, NaCl, L-glucose, and o-methyl-d-glucopyranose). RRMEC exposed to o-methyl-d-glucopyranose (a non-metabolizable glucose analogue) for 6 days caused a significant decrease in the mean band density of syndecan-3 (28%, $p<0.05$; Fig. 6B) and a significant increase in the Western blot intensity of CD44 (72%, $p<0.01$; Fig. 6D). However, exposure to o-methyl-d-glucopyranose did not lead to significant changes in the expression of syndecan-1 (Fig. 6A) or glypican-1 (Fig. 6C). Furthermore, no substantial changes were observed in the expression of syndecan-1, syndecan-3, glypican-1, or CD44 when RRMEC

were treated with mannitol, NaCl, or L-glucose (Fig. 6A–D). The results indicate that independent of its higher osmolarity, hyperglycemia can cause changes in the expression of syndecan-1 and glypican-1. However, osmolarity may have a possible, but not definitive, role in the loss of syndecan-3 and increase in CD44 expression in RRMEC in response to high glucose.

3.7 Effect of hyperglycemia on the expression of syndecan-2, syndecan-4, glypican-3, and glypican-4 in RRMEC

Treatment with high glucose for 6 days led to a significant increase in mRNA levels of both syndecan-2 (47%, $p < 0.01$; Fig. 7A) and syndecan-4 (26%, $p < 0.05$; Fig. 7B) in RRMEC. Further, mass spectrometry analysis suggested a significant increase in the protein intensity of syndecan-4 in RRMEC exposed to high glucose compared to normal glucose conditions (37%, $p < 0.01$; Fig. 7C). Interestingly, the mass spectrometry data also showed a significant decrease in protein levels of glypican-3 (47%, $p < 0.01$; Fig. 8A), but no changes in glypican-4 levels (Fig. 8B). A description of MS results is provided in Table 1. We were not able to detect quantifiable amounts of syndecan-1, -2, -3 or glypican-1 using MS. We also found a significant increase in the mRNA level of glypican-3 in RRMEC exposed to high glucose (48%, $p < 0.01$; Fig. 8C). Due to our current lack of optimum antibodies against rat syndecan-2 and syndecan-4, the confirmation of these findings using Western blot and/or immunostaining will be done in future studies, as is the case for glypican-3 and glypican-4.

4. Discussion

Diabetic retinopathy (DR) is characterized by hyperpermeability, leukocyte plugging and loss of capillaries, and neovascularization. It has been demonstrated that the systemic loss of glycocalyx occurs in diabetes, and the loss of retinal glycocalyx may contribute to the microvascular complications of DR. Previously, both diabetic animals and diabetic patients have shown a significant reduction of glycocalyx thickness in the retina. However, virtually nothing is known about how the components of the retinal glycocalyx are affected by diabetes, except for one study that showed a significant reduction in the synthesis of heparan sulfate in diabetic rats. To our knowledge, this is the first report of hyperglycemia-induced changes in the synthesis, expression, and shedding of syndecan-1, syndecan-3, glypican-1, and CD44. In this study, we describe a number of novel observations of changes in glycocalyx molecules in the retina after 8 weeks of hyperglycemia, including (1) a decrease in mRNA levels of syndecan-3, (2) an increase in mRNA levels of syndecan-1, glypican-1, and CD44, (3) a significant reduction in the protein expression of syndecan-3, (4) an increase in protein levels of syndecan-1, (5) a decrease in glypican-1 protein levels in endothelial cells *in vitro*, but an increase in the retinas of diabetic rats *in vivo*, (6) an increase in protein levels of CD44 in endothelial cells *in vitro*, but a decrease in the retinas of diabetic rats *in vivo*, and (7) an increase in systemic shedding of syndecan-1 and CD44. It is possible that future studies can be designed based on our observational results to identify whether changes in the glycocalyx are associated with the progression of DR.

The loss of cellular syndecan-1 levels and an increase in soluble syndecan-1 correlate with reduced junctional protein expression and transendothelial/epithelial cell resistance under

hyperglycemic conditions, suggesting that syndecan-1 plays a role in regulating permeability (Qing et al., 2015). Hyperpermeability is a major hallmark of DR. Previously, it was shown that RRMECs grown under high glucose conditions exhibit a significant increase in permeability (Eshaq & Harris, 2020). Further, retinal vasculature permeability increases significantly in STZ-induced rats as early as 1 week and remains elevated through 1, 4, 8, 9, and 12 months (Lawson et al., 2005; Li, Hui, Yan, & Du, 2007; Naderi, Zahed, Aghajanjpour, Amoli, & Lashay, 2019; Y. L. Wang et al., 2015). Syndecan-1 is linked to the cytoskeleton, where it mediates flow-induced elongation and alignment of endothelial cells (Ebong et al., 2014). In the ocular vasculature, syndecan-1 inhibits leukocyte-endothelial interactions and angiogenesis (Götte et al., 2002). Given these roles of syndecan-1, a substantial increase in its expression in both RRMEC and rat retinas under hyperglycemic conditions may initiate compensatory protective mechanisms. However, syndecan-1 has also been shown to be expressed on rod photoreceptor cells, glial cells, bipolar cells, and horizontal cells (Atlas). Therefore, our retinal findings cannot be attributed to endothelial cells only, but to our knowledge, the effect of high glucose on syndecan-1 expression on other types of retinal cells has not yet been determined. Future studies using either immunofluorescence or endothelial cell isolation may help determine whether our findings are specific to endothelial cells. Contrary to our findings, other studies have shown that high-glucose stimulation caused a significant loss of syndecan-1 in intestinal epithelial cells, intestinal tissue, human umbilical vein endothelial cells, and human renal glomerular endothelial cells (Gharagozlian et al., 2006; Qing et al., 2015; Qiu et al., 2010). However, no changes were observed in syndecan-1 following high-glucose treatment in bovine aortic endothelial cells (Lopez-Quintero et al., 2013). Oxidative stress, a major pathological event in diabetes, has been shown to increase mRNA levels of syndecan-1 in human adipose microvascular endothelial cells (Ali, Mahmoud, Le Master, Levitan, & Phillips, 2019). This disparity between syndecan-1 changes in response to hyperglycemia indicates tissue-specific responses.

We further observed an increase in shedding of syndecan-1 in cell culture supernatants and the plasma of diabetic rats. As mentioned above, a significant loss of syndecan-1 is observed in intestinal and renal glomerular endothelial cells in hyperglycemia, and therefore, multiple tissues may be contributing sources of soluble syndecan-1 in the plasma. Previously, an increase in serum levels of syndecan-1 was detected in both diabetic patients and STZ-induced diabetic animals (Qing et al., 2015; J. B. Wang et al., 2009; J. B. Wang et al., 2013). In addition, vitreous levels of syndecan-1 escalated in proliferative diabetic retinopathy (PDR) patients, suggesting increased shedding of syndecan-1 (Abu El-Asrar et al., 2015). However, circulating levels of syndecan-1 decreased in db/db mice (Hirota, Levy, & Iba, 2020). Several sheddases, including MMP-2, MMP-7, MMP-9, and ADAM17, can cleave syndecan-1 (Ali et al., 2019; Hayashida, Stahl, & Park, 2008; Pruessmeyer et al., 2010; Szatmári & Dobra, 2013; Zeng, Adamson, Curry, & Tarbell, 2014) and some have been shown to increase in diabetes (Eshaq & Harris, 2019; Kadoglou, Sailer, Fotiadis, Kapelouzou, & Liapis, 2014). Heparanase can also stimulate syndecan-1 shedding (Abu El-Asrar et al., 2015) and has been shown to be elevated in the plasma of Type 2 diabetic patients (Shafat, Ilan, Zoabi, Vlodyavsky, & Nakhoul, 2011). Shed ectodomains of syndecan-1 contain intact HS chains (Szatmári et al., 2015), therefore retaining its ability

to bind to growth factors and extracellular matrix components (Sztamári et al., 2015). VEGF can form a complex with soluble syndecan-1 and potentiate the integrin and VEGF receptors, thereby causing an increase in endothelial cell invasion and angiogenesis (Abu El-Asrar et al., 2015; Purushothaman et al., 2010). Although the role of soluble syndecan-1 in diabetic retinopathy has not yet been elucidated, we speculate that it could potentially contribute to neovascularization, the hallmark of PDR. We can further speculate that a change in localization of syndecan-1 from membrane-bound protein to soluble protein can have other pathological effects. Therefore, the increased production of syndecan-1 by retinal endothelial cells, coupled with increased shedding of syndecan-1, could possibly have a deleterious, rather than protective, effect.

On endothelial cells, syndecan-3 regulates inflammation, leukocyte adhesion, and colocalizes with tissue factor pathway inhibitors (Arokiasamy et al., 2019; Tinholt et al., 2015). In antigen-induced arthritis, membrane bound syndecan-3 drives the progression of disease and cartilage damage by binding to chemokines and recruiting leukocytes (Kehoe et al., 2014). However, soluble syndecan-3 inhibited leukocyte migration and reduced the severity of rheumatoid arthritis (Eustace et al., 2019). In addition, syndecan-3 has been shown to play anti-inflammatory roles in dermal and cremasteric vasculature (Kehoe et al., 2014). The ectodomain of syndecan-3 has anti-angiogenic properties (De Rossi & Whiteford, 2013); however, syndecan-3/-4 ectodomain fragments generated by thrombin cleavage cause endothelial barrier disruption (Jannaway, Yang, Meegan, Coleman, & Yuan, 2019), thereby causing hyperpermeability. Syndecan-3 is one of the relatively less-studied proteoglycans in the syndecan family; however, it is apparent that, similar to syndecan-1, syndecan-3 plays a paradoxical role depending on whether it is present in a membrane-bound or soluble form. In addition, syndecan-3 could exert tissue-specific effects depending on physiological/pathological state, with its role in the ocular circulation yet to be elucidated. To our knowledge, the effect of high-glucose stimulation on syndecan-3 expression has not yet been studied, and this is the first study to show a significant loss of syndecan-3 in the retina under hyperglycemic conditions. High glucose caused a significant reduction in the mRNA levels of syndecan-3, indicating that hyperglycemia inhibits the ability of the cell to produce syndecan-3. Since studies in the literature provide evidence for tissue specific roles for syndecan-3, it would be interesting to know whether the loss of syndecan-3 is pathological or protective for DR. Although we found syndecan-3 on RRMECs, it should be noted that it is also expressed on neuronal (bipolar and photoreceptor cells) and Müller glial cells in the retina (Atlas).

Glypican-1, a GPI-anchored proteoglycan, is anchored to caveolae in which endothelial nitric oxide synthase (eNOS) resides and regulates shear stress-induced eNOS activation, functioning as a primary mechanosensor (Bartosch et al., 2017; Zeng & Liu, 2016). Glypican-1 senses flow and initiates PECAM-1 phosphorylation, which leads to eNOS phosphorylation and nitric oxide production (Bartosch et al., 2017). In addition, as glypican-1 has been shown to regulate endothelial cell growth (Monteforte et al., 2016; Qiao, Meyer, Mundhenke, Drew, & Friedl, 2003; Qiao, Yang, Meyer, & Friedl, 2008) and VEGF165 activity (Gengrinovitch et al., 1999), it may play a crucial role in angiogenesis. RRMEC cultured in high glucose exhibited a significant increase in mRNA levels but a significant decrease in protein levels of glypican-1. We did not observe any differences

in shedding of glypican-1 between normal glucose and high-glucose conditions; therefore, instead of increased shedding, we speculate that there is either a reduction in protein synthesis or an elevation of ubiquitin proteolysis of glypican-1 in retinal endothelial cells treated with high glucose. Diabetic rats also showed a significant increase in mRNA levels of glypican-1, but contrary to our findings *in vitro*, the protein expression of glypican-1 increased significantly in the retinas of diabetic rats. In the retina, glypican-1 is expressed on neuronal cells (bipolar, horizontal, and photoreceptor cells), Müller glia cells, and vascular cells (Atlas). Therefore, the difference between our findings *in vitro* and *in vivo* may be due to differential expression of glypican-1 in different cell types in the retina. A significant increase in expression of glypican-1 was detected in cardiac tissue of STZ-diabetic rats, which correlated with diastolic dysfunction (Strunz et al., 2017). We speculate that the loss of glypican-1 may be specific to endothelial cells, but future experiments are required to confirm this. Previously, stimulation of human renal glomerular endothelial cells with high glucose led to a significant decrease in both mRNA and protein levels of glypican-1 (Qiu et al., 2010). A substantial loss of glypican-1 has also been observed in dermal vasculature (Monteforte et al., 2016). However, no changes were observed in glypican-1 levels in bovine aortic endothelial cells treated with high glucose (Lopez-Quintero et al., 2013). Glypican-1 is a primary mechanosensor; its loss can reduce nitric oxide levels, which causes further endothelial dysfunction and inflammation, thereby potentially contributing to the progression of DR (Endemann & Schiffrin, 2004).

CD44 plays a major role in endothelial cell proliferation, immune cell migration and activation, and angiogenesis (Hasib et al., 2019). In the retina, CD44 mediates photoreceptor and interphotoreceptor matrix formation and retinal angiogenesis (Chen et al., 2020). Advanced glycation products, a hallmark of diabetes, have been shown to increase the interaction between moesin and CD44 in primary retinal microvascular pericytes. Moesin links actin filaments to membrane proteins such as CD44, thereby regulating cell shape and migration. The increased interaction of moesin and CD44 can stimulate pericyte migration and detachment, which can potentiate neovascularization (Zhang et al., 2020). In addition, CD44 is a marker for mesenchymal stem cells (Tang et al., 2012), and increased CD44 levels suggest endothelial-mesenchymal transition (EndMT). EndMT can result in increased endothelial cell invasion and migration, leading ultimately to pathological angiogenesis (Thomas et al., 2019). We observed a significant increase in both mRNA and protein levels of CD44 in RRMEC under hyperglycemic conditions. Previously, retinal degeneration has been shown to increase both mRNA transcripts and protein expression of CD44 (Krishnamoorthy, Agarwal, & Chaitin, 2000). The increase in CD44 expression is implicated in the progression of insulin resistance in Type 2 diabetes (Kodama et al., 2012). While expression of CD44 remained unchanged in an ECV-304 cell line treated with high glucose (Yevdokimova & Komisarenko, 2004), the ECV-304 cell line is considered inappropriate for use in studying endothelial cell biology (Brown et al., 2000).

Our findings suggest that retinal endothelial cells are producing more CD44 in response to hyperglycemic conditions. Diabetic rats exhibited a significant increase in mRNA levels of CD44, but a significant decrease in protein expression of CD44. There are two major possibilities for the disparity in our findings *in vitro* and *in vivo*: (i) the loss of CD44 *in vivo* is not specific to endothelial cells, or (ii) other plasma or tissue factors are

contributing to the loss of CD44 in the retina. CD44 is expressed by many cell types in the retina, including retinal Müller glia cells, pericytes, retinal pigment epithelial cells, and endothelial cells (Chen et al., 2020). Pericyte loss is a major pathological event that triggers neovascularization; a decrease in total CD44 may be a consequence of pericyte loss. However, we found a significant elevation in shed CD44 in both culture media and the plasma of diabetic rats, suggesting increased shedding of CD44. Therefore, it is possible that plasma factors such as MMP-9, MT1-MMP, MMP-14, ADAM10, and ADAM17 can cause the loss of CD44 *in vivo* (Nakamura et al., 2004; Stamenkovic & Yu, 2009). Previously, serum CD44 levels have been shown to be elevated in Type 2 diabetes (Kodama et al., 2012). Soluble CD44 can potentiate the secretion of IL-1 β from macrophages, which can augment inflammation (Jang et al., 2020). Furthermore, soluble CD44 induced neuronal degeneration in glioblastoma cells (Lim et al., 2018). Additional experiments are required to determine where CD44 is lost from the retina, which may elucidate the effect of CD44 loss on DR progression. Furthermore, the consequences of increased expression and shedding of CD44 are yet to be determined.

Glucose-related hyperosmolarity can promote endothelial cell angiogenesis and retinopathy progression (Madonna et al., 2016). Therefore, to examine the effect of osmotic stress on the endothelial glycocalyx components, monolayers were grown in different hyperosmotic solutions. Mannitol, NaCl, and L-glucose showed no effect on glycocalyx components. However, o-methyl-d-glucopyranose decreased syndecan-3 and increased CD44 levels, suggesting that hyperosmolarity can be a contributing, but not a definitive, factor in the changes observed in glycocalyx components. Previously, o-methyl-d-glucopyranose was shown to cause upregulation of glucose-responsive genes, including TXNIP and LPK, in hepatocytes (Svoboda et al., 2013).

Treatment with high glucose for 6 days led to a significant increase in mRNA levels of syndecan-2, syndecan-4, and glypican-3 in RRMEC. The confirmation of these findings using Western blot and/or immunostaining requires future experiments. Syndecan-4 expression is reported to increase in isolated glomeruli and cardiac tissues in Type 1 diabetic animals (Ramnath et al., 2020; Strunz et al., 2017). Both syndecan-2 and syndecan-4 have been shown to regulate angiogenesis (Corti et al., 2019; De Rossi et al., 2021; Wu, Chen, Chen, Xie, & Xu, 2018). Therefore, increased expression of both can promote neovascularization and drive the progression of DR. To our knowledge, the role of glypican-3 in endothelial cells has not yet been established, nor has the effect of hyperglycemia on protein expression of glypican-3 been tested.

A limitation of our study that will require further experiments is immunostaining of glycocalyx molecules to identify changes in the specific cellular localization under diabetic conditions. The changes observed in the retinal tissue cannot be attributed to specific cell types, especially for glypican-1 and CD44. The identification of localized changes will help design mechanistic studies to identify the molecules responsible for changes in endothelial surface molecules.

In conclusion, we detected a significant increase in soluble syndecan-1 and CD44 under high-glucose conditions, which can promote pathways related to inflammation, neuron

degradation, and neovascularization, ultimately driving the progression of disease. Our study suggests that, while syndecan-3 and CD44 were lost from the retinas of diabetic rats, the expression of syndecan-1 was significantly increased. The expression of glypican-1 decreased significantly following high-glucose treatment in RRMEC; however, it increased significantly in the retinas of diabetic rats, indicating an endothelial cell-specific loss of glypican-1. The summary of our findings is listed in Table 2.

Supplementary Material

Refer to Web version on PubMed Central for supplementary material.

Acknowledgements

The funding was provided by National Institute of Health (NIH) grants, EY025632, HL139755, and a Malcolm Feist Predoctoral Fellowship from the Center for Cardiovascular Diseases and Science (CCDS), LSU Health Shreveport.

References:

- Abu El-Asrar AM, Alam K, Nawaz MI, Mohammad G, Van den Eynde K, Siddiquei MM, ... Opendakker G (2015). Upregulated Expression of Heparanase in the Vitreous of Patients With Proliferative Diabetic Retinopathy Originates From Activated Endothelial Cells and Leukocytes. *Invest Ophthalmol Vis Sci*, 56(13), 8239–8247. doi:10.1167/iovs.15-18025 [PubMed: 26720478]
- ADA. Statistic About Diabetes. Retrieved from <https://www.diabetes.org/resources/statistics/statistics-about-diabetes>
- Ali MM, Mahmoud AM, Le Master E, Levitan I, & Phillips SA (2019). Role of matrix metalloproteinases and histone deacetylase in oxidative stress-induced degradation of the endothelial glycocalyx. *Am J Physiol Heart Circ Physiol*, 316(3), H647–H663. doi:10.1152/ajpheart.00090.2018 [PubMed: 30632766]
- Arokiasamy S, Balderstone MJM, De Rossi G, & Whiteford JR (2019). Syndecan-3 in Inflammation and Angiogenesis. *Front Immunol*, 10, 3031. doi:10.3389/fimmu.2019.03031 [PubMed: 31998313]
- Atlas HP GPC1. Retrieved from <https://www.proteinatlas.org/ENSG00000063660-GPC1/celltype>
- Atlas HP SDC1. Retrieved from <https://www.proteinatlas.org/ENSG00000115884-SDC1/celltype>
- Atlas HP SDC3. Retrieved from <https://www.proteinatlas.org/ENSG00000162512-SDC3/celltype>
- Bartosch AMW, Mathews R, & Tarbell JM (2017). Endothelial Glycocalyx-Mediated Nitric Oxide Production in Response to Selective AFM Pulling. *Biophys J*, 113(1), 101–108. doi:10.1016/j.bpj.2017.05.033 [PubMed: 28700908]
- Bollineni JS, Alluru I, & Reddi AS (1997). Heparan sulfate proteoglycan synthesis and its expression are decreased in the retina of diabetic rats. *Curr Eye Res*, 16(2), 127–130. doi:10.1076/ceyr.16.2.127.5089 [PubMed: 9068943]
- Broekhuizen LN, Lemkes BA, Mooij HL, Meuwese MC, Verberne H, Holleman F, ... Vink H (2010). Effect of sulodexide on endothelial glycocalyx and vascular permeability in patients with type 2 diabetes mellitus. *Diabetologia*, 53(12), 2646–2655. doi:10.1007/s00125-010-1910-x [PubMed: 20865240]
- Brown J, Reading SJ, Jones S, Fitchett CJ, Howl J, Martin A, ... Brown CA (2000). Critical evaluation of ECV304 as a human endothelial cell model defined by genetic analysis and functional responses: a comparison with the human bladder cancer derived epithelial cell line T24/83. *Lab Invest*, 80(1), 37–45. doi:10.1038/labinvest.3780006 [PubMed: 10653001]
- Cabrales P, Vazquez BY, Tsai AG, & Intaglietta M (2007). Microvascular and capillary perfusion following glycocalyx degradation. *J Appl Physiol* (1985), 102(6), 2251–2259. doi:10.1152/jappphysiol.01155.2006 [PubMed: 17347383]
- CDC. Put the Brakes on Diabetes Complications. Retrieved from <https://www.cdc.gov/diabetes/library/features/prevent-complications.html>

- Chen L, Fu C, Zhang Q, He C, Zhang F, & Wei Q (2020). The role of CD44 in pathological angiogenesis. *FASEB J*, 34(10), 13125–13139. doi:10.1096/fj.202000380RR [PubMed: 32830349]
- Constantinescu AA, Vink H, & Spaan JA (2003). Endothelial cell glycocalyx modulates immobilization of leukocytes at the endothelial surface. *Arterioscler Thromb Vasc Biol*, 23(9), 1541–1547. doi:10.1161/01.ATV.0000085630.24353.3D [PubMed: 12855481]
- Corti F, Wang Y, Rhodes JM, Atri D, Archer-Hartmann S, Zhang J, ... Simons M (2019). Publisher Correction: N-terminal syndecan-2 domain selectively enhances 6-O heparan sulfate chains sulfation and promotes VEGFA. *Nat Commun*, 10(1), 2124. doi:10.1038/s41467-019-10205-0 [PubMed: 31064993]
- Cox J, Hein MY, Lubner CA, Paron I, Nagaraj N, & Mann M (2014). Accurate proteome-wide label-free quantification by delayed normalization and maximal peptide ratio extraction, termed MaxLFQ. *Mol Cell Proteomics*, 13(9), 2513–2526. doi:10.1074/mcp.M113.031591 [PubMed: 24942700]
- Cox J, & Mann M (2008). MaxQuant enables high peptide identification rates, individualized p.p.b.-range mass accuracies and proteome-wide protein quantification. *Nat Biotechnol*, 26(12), 1367–1372. doi:10.1038/nbt.1511 [PubMed: 19029910]
- De Rossi G, Vähätupa M, Cristante E, Arokiasamy S, Liyanage SE, May U, ... Whiteford JR (2021). Pathological Angiogenesis Requires Syndecan-4 for Efficient VEGFA-Induced VE-Cadherin Internalization. *Arterioscler Thromb Vasc Biol*, 41(4), 1374–1389. doi:10.1161/ATVBAHA.121.315941 [PubMed: 33596666]
- De Rossi G, & Whiteford JR (2013). A novel role for syndecan-3 in angiogenesis. *F1000Res*, 2, 270. doi:10.12688/f1000research.2-270.v1 [PubMed: 24555114]
- Ebong EE, Lopez-Quintero SV, Rizzo V, Spray DC, & Tarbell JM (2014). Shear-induced endothelial NOS activation and remodeling via heparan sulfate, glypican-1, and syndecan-1. *Integr Biol (Camb)*, 6(3), 338–347. doi:10.1039/c3ib40199e [PubMed: 24480876]
- Endemann DH, & Schiffrin EL (2004). Nitric oxide, oxidative excess, and vascular complications of diabetes mellitus. *Curr Hypertens Rep*, 6(2), 85–89. doi:10.1007/s11906-004-0081-x [PubMed: 15010009]
- Eshaq RS, & Harris NR (2019). Loss of Platelet Endothelial Cell Adhesion Molecule-1 (PECAM-1) in the Diabetic Retina: Role of Matrix Metalloproteinases. *Invest Ophthalmol Vis Sci*, 60(2), 748–760. doi:10.1167/iovs.18-25068 [PubMed: 30793207]
- Eshaq RS, & Harris NR (2020). Hyperglycemia-induced ubiquitination and degradation of β -catenin with the loss of platelet endothelial cell adhesion molecule-1 in retinal endothelial cells. *Microcirculation*, 27(2), e12596. doi:10.1111/micc.12596 [PubMed: 31628816]
- Eustace AD, McNaughton EF, King S, Kehoe O, Kungl A, Matthey D, ... Middleton J (2019). Soluble syndecan-3 binds chemokines, reduces leukocyte migration in vitro and ameliorates disease severity in models of rheumatoid arthritis. *Arthritis Res Ther*, 21(1), 172. doi:10.1186/s13075-019-1939-2 [PubMed: 31300004]
- Gengrinovitch S, Berman B, David G, Witte L, Neufeld G, & Ron D (1999). Glypican-1 is a VEGF165 binding proteoglycan that acts as an extracellular chaperone for VEGF165. *J Biol Chem*, 274(16), 10816–10822. doi:10.1074/jbc.274.16.10816 [PubMed: 10196157]
- Gharagozlian S, Borrebaek J, Henriksen T, Omsland TK, Shegarfi H, & Kolset SO (2006). Effect of hyperglycemic condition on proteoglycan secretion in cultured human endothelial cells. *Eur J Nutr*, 45(7), 369–375. doi:10.1007/s00394-006-0608-9 [PubMed: 16810465]
- Gui F, You Z, Fu S, Wu H, & Zhang Y (2020). Endothelial Dysfunction in Diabetic Retinopathy. *Front Endocrinol (Lausanne)*, 11, 591. doi:10.3389/fendo.2020.00591 [PubMed: 33013692]
- Götte M, Jousen AM, Klein C, Andre P, Wagner DD, Hinkes MT, ... Bernfield M (2002). Role of syndecan-1 in leukocyte-endothelial interactions in the ocular vasculature. *Invest Ophthalmol Vis Sci*, 43(4), 1135–1141. [PubMed: 11923257]
- Hasib A, Hennayake CK, Bracy DP, Bugler-Lamb AR, Lantier L, Khan F, ... Kang L (2019). CD44 contributes to hyaluronan-mediated insulin resistance in skeletal muscle of high-fat-fed C57BL/6 mice. *Am J Physiol Endocrinol Metab*, 317(6), E973–E983. doi:10.1152/ajpendo.00215.2019 [PubMed: 31550181]

- Hayashida K, Stahl PD, & Park PW (2008). Syndecan-1 ectodomain shedding is regulated by the small GTPase Rab5. *J Biol Chem*, 283(51), 35435–35444. doi:10.1074/jbc.M804172200 [PubMed: 18957427]
- Hirota T, Levy JH, & Iba T (2020). The influence of hyperglycemia on neutrophil extracellular trap formation and endothelial glycocalyx damage in a mouse model of type 2 diabetes. *Microcirculation*, 27(5), e12617. doi:10.1111/micc.12617 [PubMed: 32125048]
- Jang JH, Kim DH, Lim JM, Lee JW, Jeong SJ, Kim KP, & Surh YJ (2020). Breast Cancer Cell-Derived Soluble CD44 Promotes Tumor Progression by Triggering Macrophage IL1 β Production. *Cancer Res*, 80(6), 1342–1356. doi:10.1158/00085472.CAN-19-2288 [PubMed: 31969374]
- Jannaway M, Yang X, Meegan JE, Coleman DC, & Yuan SY (2019). Thrombin-cleaved syndecan-3/-4 ectodomain fragments mediate endothelial barrier dysfunction. *PLoS One*, 14(5), e0214737. doi:10.1371/journal.pone.0214737 [PubMed: 31091226]
- Joussen AM, Murata T, Tsujikawa A, Kirchhof B, Bursell SE, & Adamis AP (2001). Leukocyte-mediated endothelial cell injury and death in the diabetic retina. *Am J Pathol*, 158(1), 147–152. doi:10.1016/S0002-9440(10)63952-1 [PubMed: 11141487]
- Kadoglou NP, Sailer N, Fotiadis G, Kapelouzou A, & Liapis CD (2014). The impact of type 2 diabetes and atorvastatin treatment on serum levels of MMP-7 and MMP-8. *Exp Clin Endocrinol Diabetes*, 122(1), 44–49. doi:10.1055/s-0033-1358762 [PubMed: 24464597]
- Kehoe O, Kalia N, King S, Eustace A, Boyes C, Reizes O, ... Middleton J (2014). Syndecan-3 is selectively pro-inflammatory in the joint and contributes to antigen-induced arthritis in mice. *Arthritis Res Ther*, 16(4), R148. doi:10.1186/ar4610 [PubMed: 25015005]
- Kodama K, Horikoshi M, Toda K, Yamada S, Hara K, Irie J, ... Butte AJ (2012). Expression-based genome-wide association study links the receptor CD44 in adipose tissue with type 2 diabetes. *Proc Natl Acad Sci U S A*, 109(18), 7049–7054. doi:10.1073/pnas.1114513109 [PubMed: 22499789]
- Krishnamoorthy R, Agarwal N, & Chaitin MH (2000). Upregulation of CD44 expression in the retina during the rds degeneration. *Brain Res Mol Brain Res*, 77(1), 125–130. doi:10.1016/S0169-328X(00)00035-8 [PubMed: 10814838]
- Kumase F, Morizane Y, Mohri S, Takasu I, Ohtsuka A, & Ohtsuki H (2010). Glycocalyx degradation in retinal and choroidal capillary endothelium in rats with diabetes and hypertension. *Acta Med Okayama*, 64(5), 277–283. doi:10.18926/amo/40502 [PubMed: 20975760]
- Lawson SR, Gabra BH, Guérin B, Neugebauer W, Nantel F, Battistini B, & Sirois P (2005). Enhanced dermal and retinal vascular permeability in streptozotocin-induced type 1 diabetes in Wistar rats: blockade with a selective bradykinin B1 receptor antagonist. *Regul Pept*, 124(1–3), 221–224. doi:10.1016/j.regpep.2004.09.002 [PubMed: 15544863]
- Leskova W, Pickett H, Eshaq RS, Shrestha B, Pattillo CB, & Harris NR (2019). Effect of diabetes and hyaluronidase on the retinal endothelial glycocalyx in mice. *Exp Eye Res*, 179, 125–131. doi:10.1016/j.exer.2018.11.012 [PubMed: 30445048]
- Leskova W, Watts MN, Carter PR, Eshaq RS, & Harris NR (2013). Measurement of retinal blood flow rate in diabetic rats: disparity between techniques due to redistribution of flow. *Invest Ophthalmol Vis Sci*, 54(4), 2992–2999. doi:10.1167/iovs.13-11915 [PubMed: 23572104]
- Li YJ, Hui YN, Yan F, & Du ZJ (2007). Up-regulation of integrin-linked kinase in the streptozotocin-induced diabetic rat retina. *Graefes Arch Clin Exp Ophthalmol*, 245(10), 1523–1532. doi:10.1007/s00417-007-0616-3 [PubMed: 17653754]
- Lim S, Kim D, Ju S, Shin S, Cho IJ, Park SH, ... Kim YK (2018). Glioblastoma-secreted soluble CD44 activates tau pathology in the brain. *Exp Mol Med*, 50(4), 1–11. doi:10.1038/s12276-017-0008-7
- Lopez-Quintero SV, Cancel LM, Pierides A, Antonetti D, Spray DC, & Tarbell JM (2013). High glucose attenuates shear-induced changes in endothelial hydraulic conductivity by degrading the glycocalyx. *PLoS One*, 8(11), e78954. doi:10.1371/journal.pone.0078954 [PubMed: 24260138]
- Madonna R, Giovannelli G, Confalone P, Renna FV, Geng YJ, & De Caterina R (2016). High glucose-induced hyperosmolarity contributes to COX-2 expression and angiogenesis: implications for diabetic retinopathy. *Cardiovasc Diabetol*, 15, 18. doi:10.1186/s12933-016-0342-4 [PubMed: 26822858]

- McClatchey PM, Schafer M, Hunter KS, & Reusch JE (2016). The endothelial glycocalyx promotes homogenous blood flow distribution within the microvasculature. *Am J Physiol Heart Circ Physiol*, 311(1), H168–176. doi:10.1152/ajpheart.00132.2016 [PubMed: 27199117]
- Monteforte AJ, Lam B, Das S, Mukhopadhyay S, Wright CS, Martin PE, ... Baker AB (2016). Glypican-1 nanoliposomes for potentiating growth factor activity in therapeutic angiogenesis. *Biomaterials*, 94, 45–56. doi:10.1016/j.biomaterials.2016.03.048 [PubMed: 27101205]
- Naderi A, Zahed R, Aghajanpour L, Amoli FA, & Lashay A (2019). Long term features of diabetic retinopathy in streptozotocin-induced diabetic Wistar rats. *Exp Eye Res*, 184, 213–220. doi:10.1016/j.exer.2019.04.025 [PubMed: 31028750]
- Nakamura H, Suenaga N, Taniwaki K, Matsuki H, Yonezawa K, Fujii M, ... Seiki M (2004). Constitutive and induced CD44 shedding by ADAM-like proteases and membrane-type 1 matrix metalloproteinase. *Cancer Res*, 64(3), 876–882. doi:10.1158/0008-5472.can-03-3502 [PubMed: 14871815]
- Nieuwdorp M, Mooij HL, Kroon J, Atasever B, Spaan JA, Ince C, ... Vink H (2006). Endothelial glycocalyx damage coincides with microalbuminuria in type 1 diabetes. *Diabetes*, 55(4), 1127–1132. doi:10.2337/diabetes.55.04.06.db05-1619 [PubMed: 16567538]
- Nieuwdorp M, van Haeften TW, Gouverneur MC, Mooij HL, van Lieshout MH, Levi M, ... Stroes ES (2006). Loss of endothelial glycocalyx during acute hyperglycemia coincides with endothelial dysfunction and coagulation activation in vivo. *Diabetes*, 55(2), 480–486. doi:10.2337/diabetes.55.02.06.db05-1103 [PubMed: 16443784]
- Noonan DM, Fulle A, Valente P, Cai S, Horigan E, Sasaki M, ... Hassell JR (1991). The complete sequence of perlecan, a basement membrane heparan sulfate proteoglycan, reveals extensive similarity with laminin A chain, low density lipoprotein-receptor, and the neural cell adhesion molecule. *J Biol Chem*, 266(34), 22939–22947. [PubMed: 1744087]
- Pruessmeyer J, Martin C, Hess FM, Schwarz N, Schmidt S, Kogel T, ... Ludwig A (2010). A disintegrin and metalloproteinase 17 (ADAM17) mediates inflammation-induced shedding of syndecan-1 and -4 by lung epithelial cells. *J Biol Chem*, 285(1), 555–564. doi:10.1074/jbc.M109.059394 [PubMed: 19875451]
- Purushothaman A, Uyama T, Kobayashi F, Yamada S, Sugahara K, Rapraeger AC, & Sanderson RD (2010). Heparanase-enhanced shedding of syndecan-1 by myeloma cells promotes endothelial invasion and angiogenesis. *Blood*, 115(12), 2449–2457. doi:10.1182/blood-2009-07-234757 [PubMed: 20097882]
- Qiao D, Meyer K, Mundhenke C, Drew SA, & Friedl A (2003). Heparan sulfate proteoglycans as regulators of fibroblast growth factor-2 signaling in brain endothelial cells. Specific role for glypican-1 in glioma angiogenesis. *J Biol Chem*, 278(18), 16045–16053. doi:10.1074/jbc.M211259200 [PubMed: 12591930]
- Qiao D, Yang X, Meyer K, & Friedl A (2008). Glypican-1 regulates anaphase promoting complex/cyclosome substrates and cell cycle progression in endothelial cells. *Mol Biol Cell*, 19(7), 2789–2801. doi:10.1091/mbc.e07-10-1025 [PubMed: 18417614]
- Qing Q, Zhang S, Chen Y, Li R, Mao H, & Chen Q (2015). High glucose-induced intestinal epithelial barrier damage is aggravated by syndecan-1 destruction and heparanase overexpression. *J Cell Mol Med*, 19(6), 1366–1374. doi:10.1111/jcmm.12523 [PubMed: 25702768]
- Qiu HY, Fan WR, Huang SM, Liu F, Tang WZ, & Zuo C (2010). [Effect of high concentration of glucose on thickness of glycocalyx and expression of syndecan-1 and glypican-1 in cultured human renal glomerular endothelial cells]. *Sichuan Da Xue Xue Bao Yi Xue Ban*, 41(6), 980–985. [PubMed: 21265098]
- Ramnath RD, Butler MJ, Newman G, Desideri S, Russell A, Lay AC, ... Satchell SC (2020). Blocking matrix metalloproteinase-mediated syndecan-4 shedding restores the endothelial glycocalyx and glomerular filtration barrier function in early diabetic kidney disease. *Kidney Int*, 97(5), 951–965. doi:10.1016/j.kint.2019.09.035 [PubMed: 32037077]
- Reitsma S, Slaaf DW, Vink H, van Zandvoort MA, & oude Egbrink MG (2007). The endothelial glycocalyx: composition, functions, and visualization. *Pflugers Arch*, 454(3), 345–359. doi:10.1007/s00424-007-0212-8 [PubMed: 17256154]
- Saeedi P, Petersohn I, Salpea P, Malanda B, Karuranga S, Unwin N, ... Committee, I. D. A. (2019). Global and regional diabetes prevalence estimates for 2019 and projections for 2030 and 2045:

- Results from the International Diabetes Federation Diabetes Atlas, 9. *Diabetes Res Clin Pract*, 157, 107843. doi:10.1016/j.diabres.2019.107843 [PubMed: 31518657]
- Shafat I, Ilan N, Zoabi S, Vlodayvsky I, & Nakhoul F (2011). Heparanase levels are elevated in the urine and plasma of type 2 diabetes patients and associate with blood glucose levels. *PLoS One*, 6(2), e17312. doi:10.1371/journal.pone.0017312 [PubMed: 21364956]
- Simó R, & Hernández C (2015). Novel approaches for treating diabetic retinopathy based on recent pathogenic evidence. *Prog Retin Eye Res*, 48, 160–180. doi:10.1016/j.preteyeres.2015.04.003 [PubMed: 25936649]
- Stamenkovic I, & Yu Q (2009). Shedding light on proteolytic cleavage of CD44: the responsible sheddase and functional significance of shedding. *J Invest Dermatol*, 129(6), 1321–1324. doi:10.1038/jid.2009.13 [PubMed: 19434087]
- Strunz CMC, Roggerio A, Cruz PL, Pacanaro AP, Salemi VMC, Benvenuti LA, ... Irigoyen MC (2017). Down-regulation of fibroblast growth factor 2 and its coreceptors heparan sulfate proteoglycans by resveratrol underlies the improvement of cardiac dysfunction in experimental diabetes. *J Nutr Biochem*, 40, 219–227. doi:10.1016/j.jnutbio.2016.11.015 [PubMed: 27951474]
- Svoboda M, Tastenoy M, Zhang Y, Gillet C, Rasschaert J, Malaisse WJ, & Sener A (2013). D-glucose- and 3-O-methyl-D-glucose-induced upregulation of selected genes in rat hepatocytes and INS1E cells: re-evaluation of the possible role of hexose phosphorylation. *Mol Med Rep*, 8(3), 829–836. doi:10.3892/mmr.2013.1582 [PubMed: 23846350]
- Szatmári T, & Dobra K (2013). The role of syndecan-1 in cellular signaling and its effects on heparan sulfate biosynthesis in mesenchymal tumors. *Front Oncol*, 3, 310. doi:10.3389/fonc.2013.00310 [PubMed: 24392351]
- Szatmári T, Ötvös R, Hjerpe A, & Dobra K (2015). Syndecan-1 in Cancer: Implications for Cell Signaling, Differentiation, and Prognostication. *Dis Markers*, 2015, 796052. doi:10.1155/2015/796052 [PubMed: 26420915]
- Tang R, Gao M, Wu M, Liu H, Zhang X, & Liu B (2012). High glucose mediates endothelial-to-chondrocyte transition in human aortic endothelial cells. *Cardiovasc Diabetol*, 11, 113. doi:10.1186/1475-2840-11-113 [PubMed: 22998723]
- Thomas AA, Biswas S, Feng B, Chen S, Gonder J, & Chakrabarti S (2019). lncRNA H19 prevents endothelial-mesenchymal transition in diabetic retinopathy. *Diabetologia*, 62(3), 517–530. doi:10.1007/s00125-018-4797-6 [PubMed: 30612136]
- Tinholt M, Stavik B, Louch W, Carlson CR, Sletten M, Ruf W, ... Iversen N (2015). Syndecan-3 and TFPI colocalize on the surface of endothelial-, smooth muscle-, and cancer cells. *PLoS One*, 10(1), e0117404. doi:10.1371/journal.pone.0117404 [PubMed: 25617766]
- Tkachenko E, Rhodes JM, & Simons M (2005). Syndecans: new kids on the signaling block. *Circ Res*, 96(5), 488–500. doi:10.1161/01.RES.0000159708.71142.c8 [PubMed: 15774861]
- Vink H, Constantinescu AA, & Spaan JA (2000). Oxidized lipoproteins degrade the endothelial surface layer : implications for platelet-endothelial cell adhesion. *Circulation*, 101(13), 1500–1502. doi:10.1161/01.cir.101.13.1500 [PubMed: 10747340]
- Wang JB, Guan J, Shen J, Zhou L, Zhang YJ, Si YF, ... Sheng Y (2009). Insulin increases shedding of syndecan-1 in the serum of patients with type 2 diabetes mellitus. *Diabetes Res Clin Pract*, 86(2), 83–88. doi:10.1016/j.diabres.2009.08.002 [PubMed: 19735958]
- Wang JB, Zhang YJ, Zhang Y, Guan J, Chen LY, Fu CH, ... Si YF (2013). Negative correlation between serum syndecan-1 and apolipoprotein A1 in patients with type 2 diabetes mellitus. *Acta Diabetol*, 50(2), 111–115. doi:10.1007/s00592-010-0216-2 [PubMed: 20683626]
- Wang W, & Lo ACY (2018). Diabetic Retinopathy: Pathophysiology and Treatments. *Int J Mol Sci*, 19(6). doi:10.3390/ijms19061816
- Wang YL, Wang K, Yu SJ, Li Q, Li N, Lin PY, ... Guo JY (2015). Association of the TLR4 signaling pathway in the retina of streptozotocin-induced diabetic rats. *Graefes Arch Clin Exp Ophthalmol*, 253(3), 389–398. doi:10.1007/s00417-014-2832-y [PubMed: 25359392]
- Wright WS, Eshaq RS, Lee M, Kaur G, & Harris NR (2020). Retinal Physiology and Circulation: Effect of Diabetes. *Compr Physiol*, 10(3), 933–974. doi:10.1002/cphy.c190021 [PubMed: 32941691]

- Wu H, Chen Z, Chen JZ, Xie J, & Xu B (2018). Resveratrol Improves Tube Formation in AGE-Induced Late Endothelial Progenitor Cells by Suppressing Syndecan-4 Shedding. *Oxid Med Cell Longev*, 2018, 9045976. doi:10.1155/2018/9045976
- Yevdokimova NY, & Komisarenko SV (2004). TGFbeta1 is involved in high glucose-induced accumulation of pericellular chondroitin sulphate in human endothelial cells. *J Diabetes Complications*, 18(5), 300–308. doi:10.1016/S1056-8727(03)00113-2 [PubMed: 15337504]
- Zeng Y, Adamson RH, Curry FR, & Tarbell JM (2014). Sphingosine-1-phosphate protects endothelial glycocalyx by inhibiting syndecan-1 shedding. *Am J Physiol Heart Circ Physiol*, 306(3), H363–372. doi:10.1152/ajpheart.00687.2013 [PubMed: 24285115]
- Zeng Y, & Liu J (2016). Role of glypican-1 in endothelial NOS activation under various steady shear stress magnitudes. *Exp Cell Res*, 348(2), 184–189. doi:10.1016/j.yexcr.2016.09.017 [PubMed: 27688027]
- Zhang SS, Hu JQ, Liu XH, Chen LX, Chen H, Guo XH, & Huang QB (2020). Role of Moesin Phosphorylation in Retinal Pericyte Migration and Detachment Induced by Advanced Glycation Endproducts. *Front Endocrinol (Lausanne)*, 11, 603450. doi:10.3389/fendo.2020.603450 [PubMed: 33312163]

Highlights

- High glucose causes a diversity of changes in the retinal/endothelial glycocalyx.
- Syndecan-3 mRNA and protein are decreased from retinal cells in hyperglycemia.
- Plasma levels of shed syndecan-1 and CD44 are increased in diabetic rats.
- Glypican-1 mRNA increases in hyperglycemic retinal endothelial cells.
- Increases of some glycocalyx components may be compensatory for the overall loss.

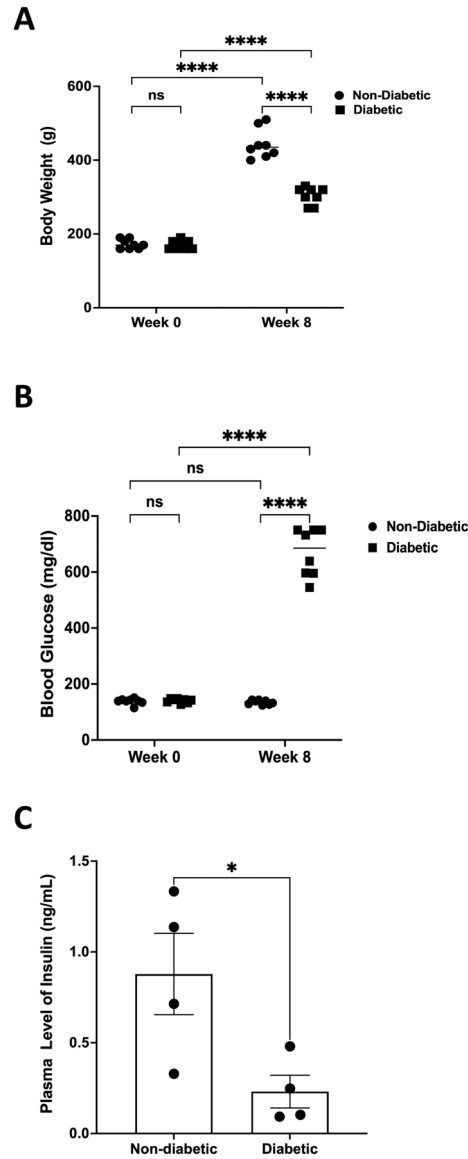


Figure 1. Body weight, blood glucose, and insulin levels.

(A) STZ-induced diabetes significantly slowed weight gain in rats. After 8 weeks of hyperglycemia, the body weight of diabetic rats was significantly less ($****p<0.0001$, $n=8$) compared to that of their non-diabetic counterparts. (B) Blood glucose was significantly higher ($****p<0.0001$, $n=8$) in diabetic rats compared to controls, while plasma insulin levels were significantly decreased ($*p<0.05$, $n=4$) in diabetic rats (C). The medians of body weights and glucose measurements are indicated. Insulin values are represented as mean \pm SEM. ns = non-significant.

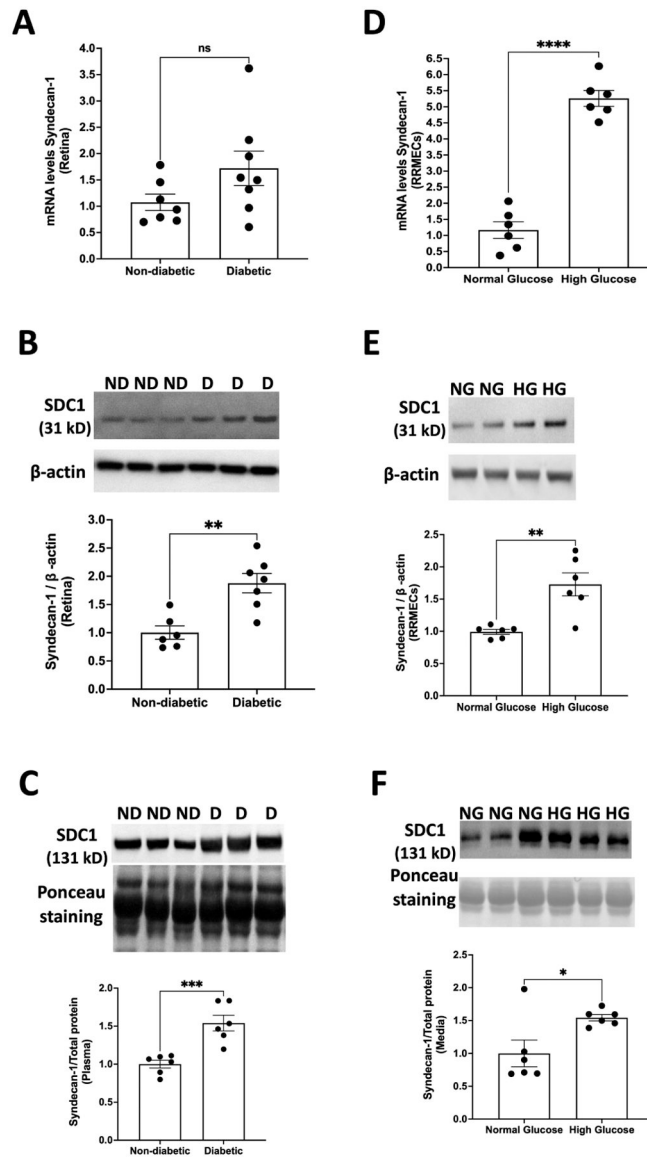


Figure 2. Effect of high glucose on syndecan-1.

(A) mRNA levels of syndecan-1 tended to increase in the retinas of diabetic rats ($p=0.11$, $n=7-8$). In addition, diabetic rats exhibited a significant increase in (B) the protein expression of syndecan-1 in the retina (** $p<0.01$, $n=6-7$) and (C) plasma levels of syndecan-1 (** $p<0.001$, $n=6$). RRMEC grown under high-glucose conditions showed a significant increase in both (D) mRNA (**** $p<0.0001$, $n=6$) and (E) protein levels (** $p<0.01$, $n=6$) of syndecan-1. (F) Elevated levels of syndecan-1 in the media were seen following high-glucose treatment (* $p<0.05$, $n=6$) under hyperglycemic conditions. Western blot data normalized to either β -actin (RRMEC and retina) or total protein (plasma and media). ND, non-diabetic; D, diabetic; NG, normal glucose; HG, high glucose. ns = non-significant.

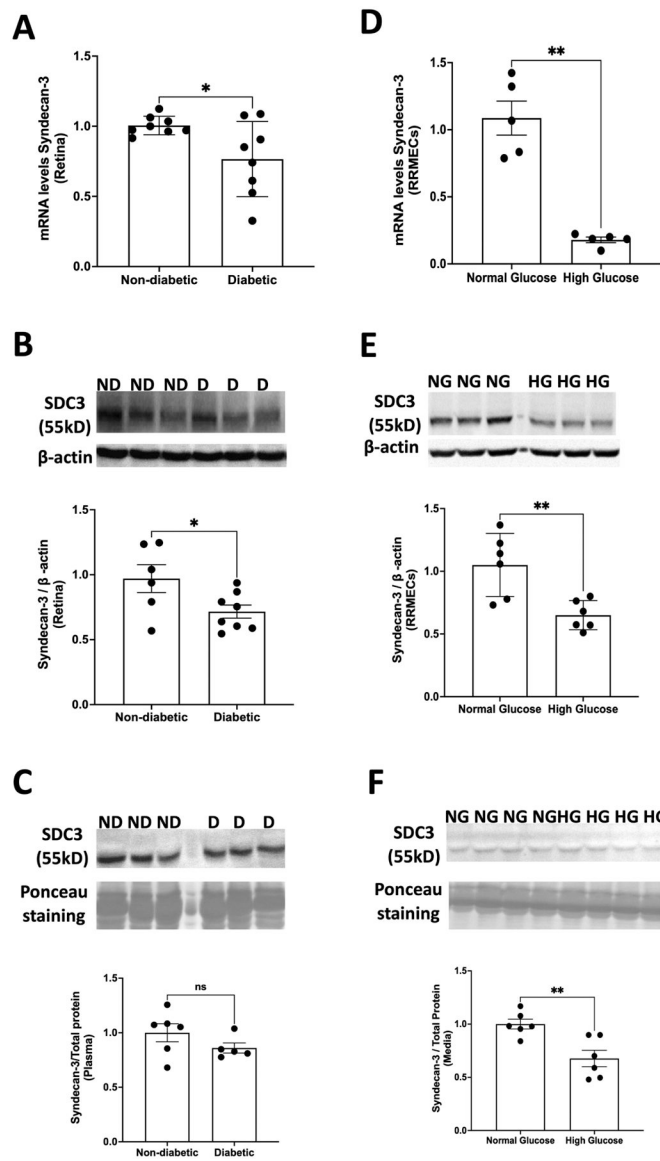


Figure 3. Effect of high glucose on syndecan-3.

(A) mRNA levels (* $p < 0.05$, $n = 8$) and (B) protein expression of syndecan-3 (* $p < 0.05$, $n = 6-8$) decreased significantly in the retinas of diabetic rats. However, no changes were observed in the plasma levels of syndecan-3 in diabetic vs non-diabetic animals ($n = 5-6$). (C) The exposure of RRMEC to high glucose for 6 days also caused a significant decrease in both (D) mRNA (** $p < 0.01$, $n = 6$) and (E) protein levels (** $p < 0.01$, $n = 6$) of syndecan-3. (F) The media levels of syndecan-3 decreased significantly (** $p < 0.01$, $n = 6$) under hyperglycemic conditions. ns = non-significant.

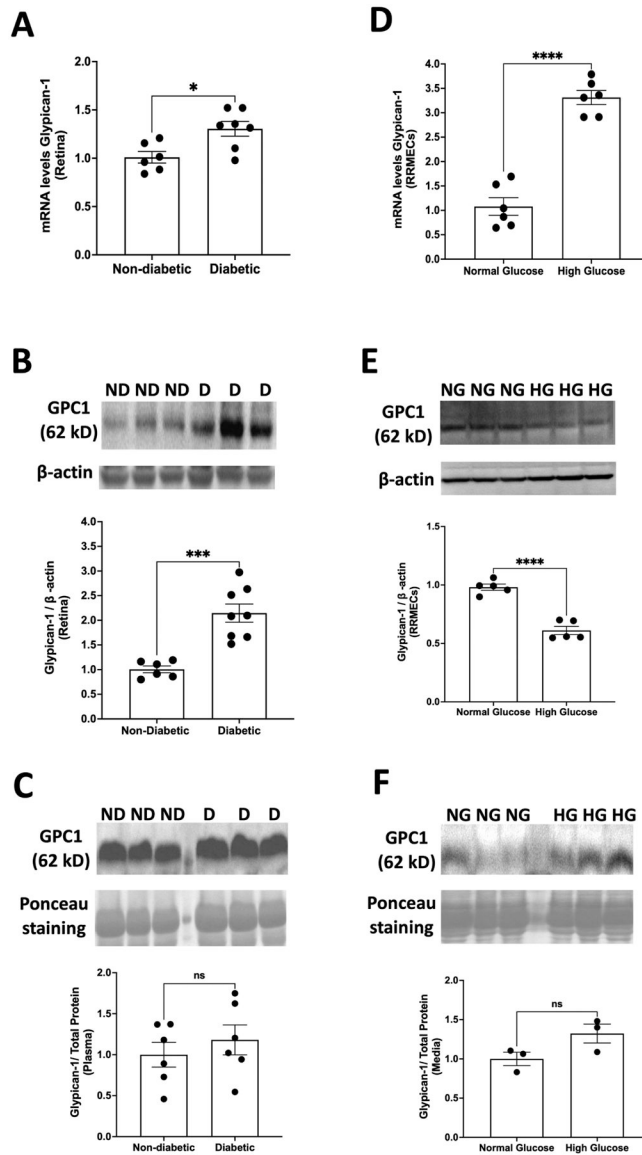


Figure 4. Effect of high glucose on glypican-1.

Eight weeks of diabetes caused significant increases in both (A) mRNA levels ($*p < 0.05$, $n = 6-7$) and (B) protein levels ($***p < 0.001$, $n = 6-8$) of glypican-1 in the retinas of diabetic rats. In comparison to those exposed to normal glucose, RRMEC stimulated with high glucose exhibited a significant increase in (D) mRNA levels of glypican-1 ($****p < 0.0001$, $n = 6$); however, protein expression was significantly decreased ($****p < 0.0001$, $n = 5$) (E). No changes were observed in (C) plasma ($n = 6$) or (F) media levels ($n = 3$) of glypican-1 in normal glucose vs hyperglycemic conditions. ns = non-significant.

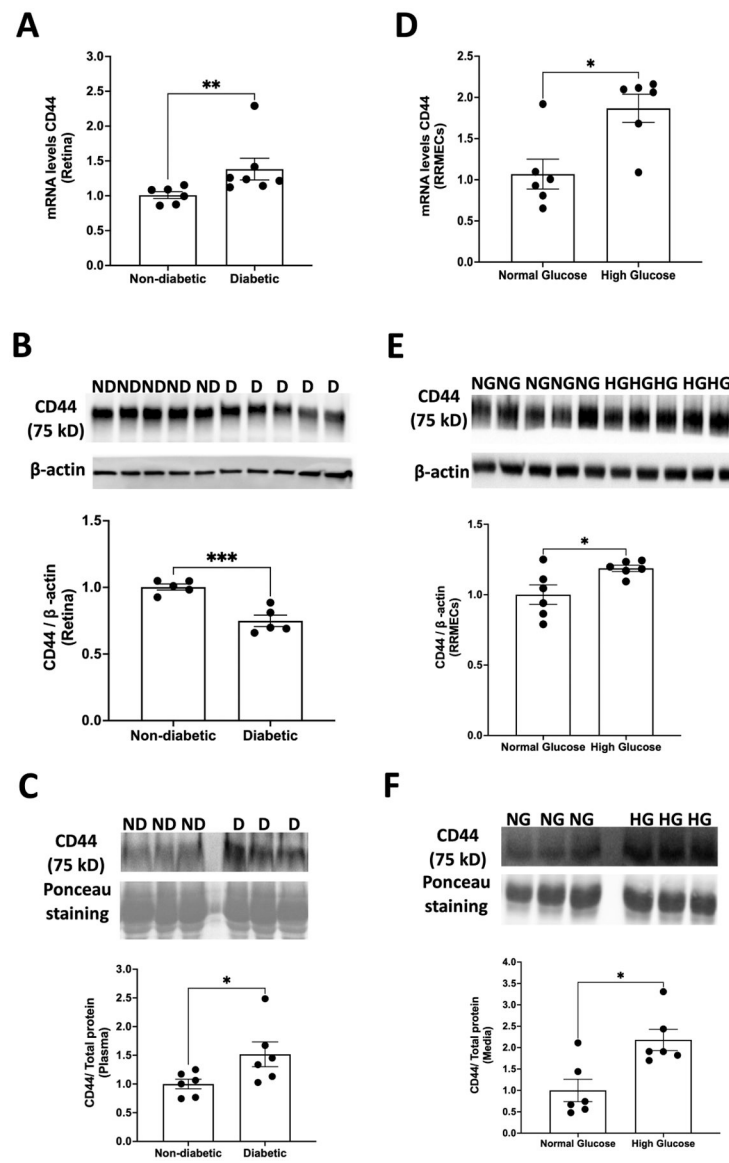


Figure 5. Effect of high glucose on CD44.

(A) A significant increase in mRNA levels of CD44 was observed in the retinas of diabetic animals (** $p < 0.01$, $n = 6-7$). However, retinal protein expression of CD44 was decreased (** $p < 0.001$, $n = 5$) in diabetic rats compared to non-diabetic rats (B). As compared to normal glucose, RRMEC treated with high glucose had a significant increase in both (D) mRNA (* $p < 0.05$, $n = 6$) and (E) protein levels (* $p < 0.05$, $n = 6$) of CD44. In addition, the (C) plasma ($n = 6$) and (F) media levels of CD44 ($n = 6$) were significantly higher ($p < 0.05$) under hyperglycemic conditions, suggesting increased shedding of CD44 in diabetes.

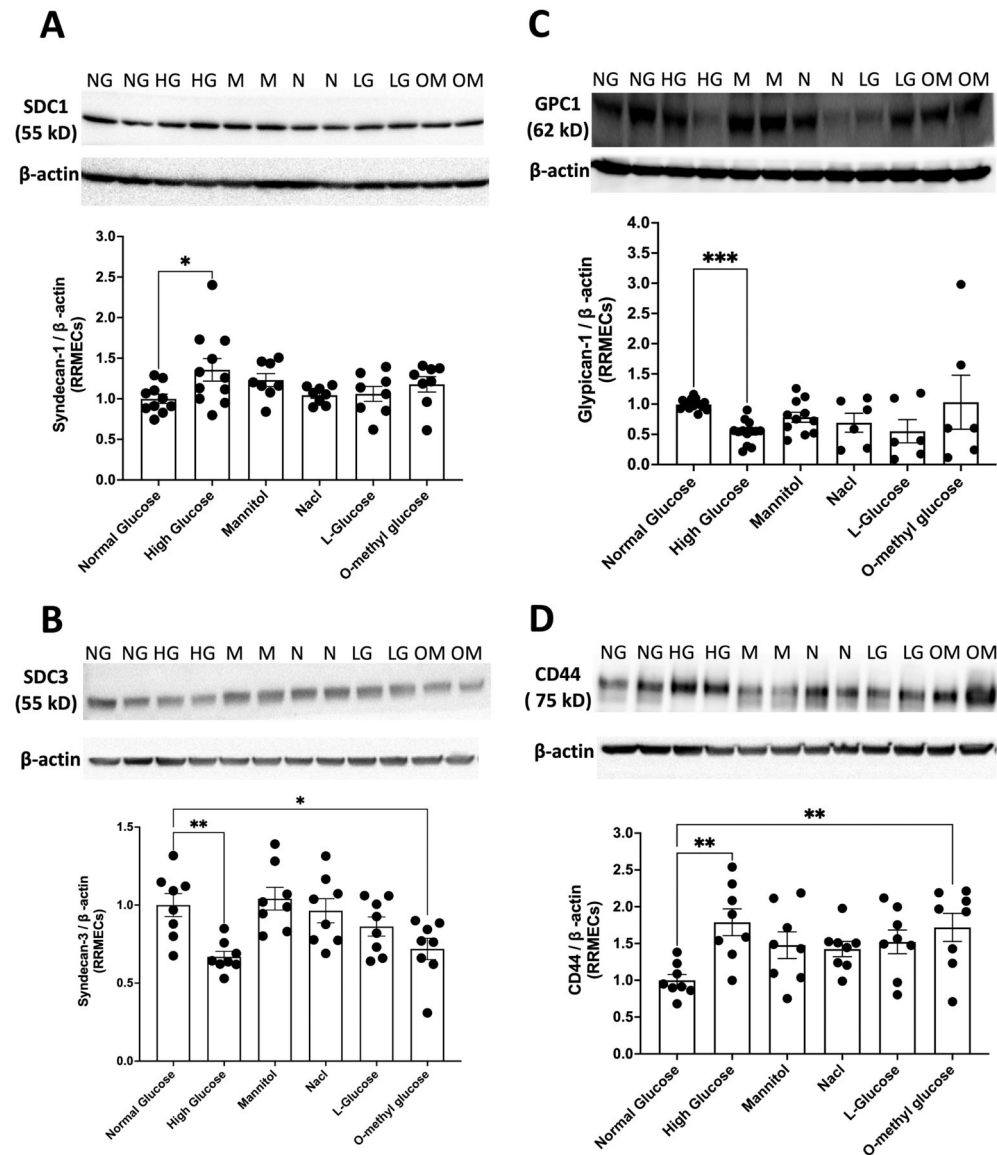


Figure 6. Effect of osmolarity on the expression of core proteins in RRMEC.

RRMEC exposure to o-methyl-d-glucopyranose for 6 days caused **(B)** a significant decrease in syndecan-3 expression (* $p < 0.05$) and **(D)** a significant increase in CD44 levels (** $p < 0.01$). However, o-methyl-d-glucopyranose exposure did not lead to any significant changes in the expression of syndecan-1 **(A)** or glypican-1 **(C)**. No substantial changes were observed in the expression of syndecan-1, syndecan-3, glypican-1, or CD44 when RRMEC were treated with mannitol, NaCl, or L-glucose. NG, normal glucose; HG, high glucose; M, mannitol; N, NaCl; LG, L-glucose; OM, o-methyl glucose, $n = 8-14$.

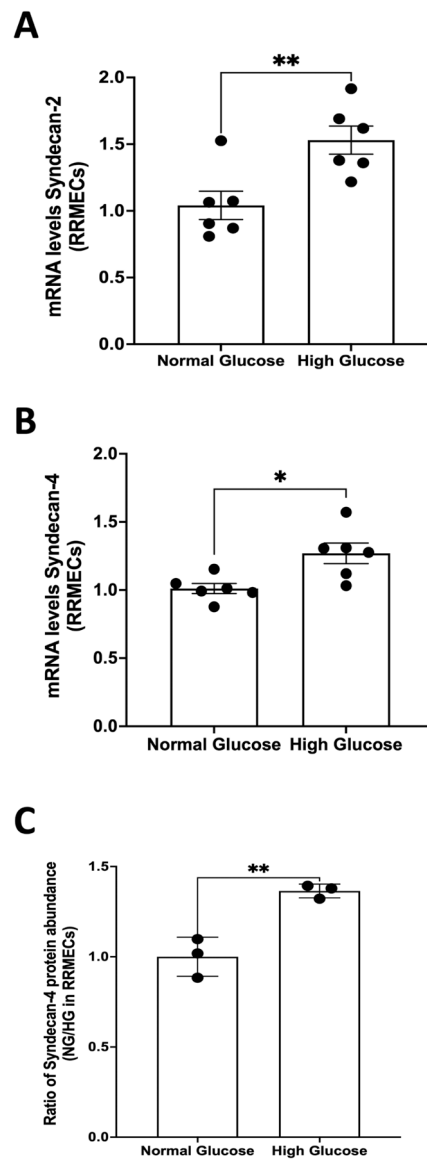


Figure 7. Effect of hyperglycemia on the expression of syndecan-2 and syndecan-4 in RRMEC. Treatment with high glucose for 6 days led to a significant increase in mRNA levels of both (A) syndecan-2 (** $p < 0.01$, $n = 6$) and (B) syndecan-4 (* $p < 0.05$, $n = 6$) in RRMEC. (C) A significant increase in the protein intensity of syndecan-4 in RRMEC exposed to high glucose (** $p < 0.01$, $n = 3$) was observed following analysis using mass spectrometry.

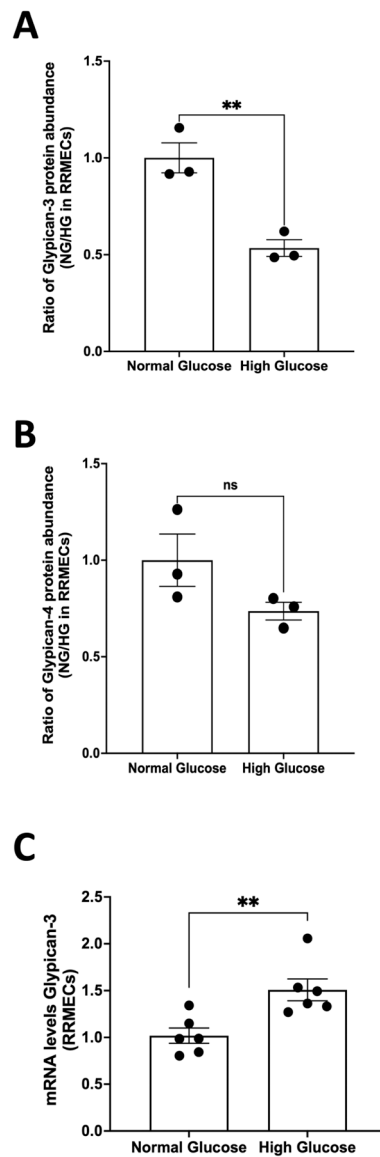


Figure 8. Effect of hyperglycemia on the expression of glypican-3 and glypican-4 in RRMEC. Mass spectrometry analyses suggested a significant reduction in the protein intensity of (A) glypican-3 (** $p < 0.01$, $n = 3$) but no change in (B) glypican-4 ($n = 3$) in RRMEC grown under high-glucose conditions. (C) mRNA levels of glypican-3 were significantly higher (** $p < 0.01$, $n = 6$) in RRMEC treated with high glucose compared to normal glucose.

Table 1.

Description of Mass Spectrometry data.

Gene Name	SDC4	GPC3	GPC4
Protein Name	Syndecan-4	Glypican-3	
Majority Protein IDs	P34901	P13265; A0A0G2KBA2	Q642B0
Protein IDs	P34901	P13265; A0A0G2KBA2	Q642B0
Molecular Weight (kDa)	21.9	67.0	62.5
Sequence Coverage (%)	51	26.1	27.6
Peptides	9	13	12
LFQ intensity_NG_1	68722000	149370000	27754000
LFQ intensity_NG_2	79177000	151150000	24208000
LFQ intensity_NG_3	85365000	188160000	37752000
LFQ intensity_HG_1	108340000	79220000	22676000
LFQ intensity_HG_2	107230000	80679000	23984000
LFQ intensity_HG_3	102770000	101030000	19392000

Table 2.

Summary of hyperglycemia-induced changes observed on the expression/levels of core proteins.

	High Glucose treated RRMECs			Type 1 Diabetic Rats		
	mRNA	Protein	Media	mRNA	Protein	Plasma
Syndecan-1	↑	↑	↑	↑ trend (p=0.11)	↑	↑
Syndecan-3	↓	↓	↓	↓	↓	no change
Glypican-1	↑	↓	no change	↑	↑	no change
CD44	↑	↑	↑	↑	↓	↑

Author Manuscript

Author Manuscript

Author Manuscript

Author Manuscript